Reexamination of the Slow Mode in Semidilute Polymer Solutions: The Effect of Solvent Quality

Junfang Li,[†] Wei Li,[‡] Hong Huo,[‡] Shizhong Luo,[†] and Chi Wu*[,†,‡]

Hefei National Laboratory for Physical Sciences at Microscale, Department of Chemical Physics, University of Science and Technology of China, Hefei, Anhu 230026, China, and Department of Chemistry, The Chinese University of Hong Kong, Shatin. N.T., Hong Kong

Received June 10, 2007; Revised Manuscript Received November 12, 2007

ABSTRACT: Dust-free semidilute and concentrated polystyrene (PS) solutions in two solvents were prepared by conventional slow evaporation and in situ living anionic polymerization that removes previously troublesome artifacts, such as dust contamination and a concentration gradient. Their dynamics was reexamined by a combination of static and dynamic laser light scattering. As expected, only one fast diffusive mode was observed in benzene (an athermal solvent for PS) up to 20% concentration (C), attributed to thermally agitated fluctuation of chain segments ("blobs") confined in a noninteracting "tube" made of its surrounding chains. In cyclohexane, whose quality as a solvent for PS decreases with the temperature in the range 32−50 °C, we observed an additional slow mode. The slow mode is enhanced as the solvent quality decreases. The scaling exponent (α_s) between its related line-width (Γ_{slow}) and the scattering vector (q), i.e., $\Gamma_{slow} \sim q^{\alpha_s}$, decreases from 3 to 0 as C increases, which suggests that the slow mode has different natures, depending on C. When C is only a few times larger than the overlap concentration (C^*) but lower than the entanglement concentration (C_e), i.e., not all the chains are entangled together, the slow mode is related to transient interchain segment−segment interaction-induced clusters. When $C/C_e > 1$, it is attributed to the confinement of each chain inside an inhomogeneous tube with a "band"-like structure due to relatively stronger segment−segment interaction near the entanglement points.

Introduction

At the overlap concentration (C^*), polymer chains start to "touch" each other and the solution enters the semidilute regime. C^* is defined as $3M/(4\pi N_A R_g^3)$ or $M/(2^{3/2} N_A R_g^3)$ or $[\eta]^{-1}$, where M, R_g, N_A, and $[\eta]$ are the molar mass, the radius of gyration, the Avogadro constant, and the intrinsic viscosity, respectively.[1,2] The difference of C^* calculated from these definitions could be as large as 5 times. On the other hand, at the entanglement concentration (C_e), polymer chains start to interwind with each other, where C_e can be estimated from the ratio of the chain length (L) and the entanglement length (L_e).[3] C_e is higher than C^*. Note that for chains shorter than L_e, they are not able to entangle with each other even at higher concentrations.

The mean-field theory can effectively describe some properties of polymer solutions over the whole concentration range but fails to explain other static and dynamic properties because of strong intra- and interchain interaction among covalently bonded monomers. De Gennes[4−6] and his co-workers used the concept of a "blob", roughly defined as the segments between two neighboring cross-linking points, and developed some scaling laws to predict various properties of semidilute solutions. In a transient gel model, there exists only one characteristic length or one dynamic process in semidilute solutions if the solvent is thermodynamically good or athermal. Namely, the thermal energy (k_BT) can only agitate one short segment of the chain so that its gravity center undergoes a random Brownian motion inside a confined volume. The static and dynamic correlation lengths (ξ_S and ξ_D) can be measured from the angular dependence of the average scattering intensity and the average cooperative diffusion coefficient (D_C), respectively, by light scattering. For a distance longer than ξ, the segment−segment interaction is "completely" screened out in an athermal solvent.[5,7,8] Previous results are well represented by two master curves: $\xi_S \sim C^{-0.72\pm0.01}$ and $\xi_D \sim C^{-0.70\pm0.01}$, slightly deviated from $\xi \sim C^{-0.75}$ predicted in theories.[1,9] These scaling relationships are sometimes used to judge whether a study of semidilute solutions is creditable.

One additional slow relaxation mode has also been observed from time to time in the intensity−intensity time correlation functions of various semidilute polymer solutions.[10−18] This additional slow mode was previously assigned to different physical origins, such as the reptation of the entire chain inside a "tube" made of its surrounding chains,[4,6] the scattering vector (q) independent relaxation of a transient network,[11,16] the q^2-dependent translational diffusion of large aggregates or even dust particles,[1,14,15,17,18] and internal motions of large transient chain clusters.[9,10] Later, it was realized that the reptation is not observable in dynamic laser light scattering (LLS) due to its nature. To rule out a possible effect of dust particles, one has to prepare a dust-free semidilute polymer solution, which is still rather difficult, if not impossible, because it is too viscous to be directly filtered. Therefore, a large volume of dust-free dilute solution is first prepared and then concentrated by slow evaporation. The whole process could take months. Even using such a painful process, one still faces a concentration gradient problem, i.e., the upper layer is likely more concentrated than the bottom layer.

Theoretically, Brochard and De Gennes[19] attributed D_C to the osmotic modulus (M_π), the elastic modulus (M_0), and the friction coefficient (ζ) as $D_C = (M_\pi + M_0)/\zeta_C$. Adam and Delsanti[16] allowed the transient gel network to relax and assigned the q-independent slow mode with a viscoelastic nature and a characteristic time (τ_r). For a time scale shorter than τ_r, the semidilute solution behaves like a gel network so that both M_π and M_0 contribute to the longitudinal modulus. For a time

* Corresponding author. The Hong Kong address should be used for all correspondence.
[†] University of Science and Technology of China.
[‡] The Chinese University of Hong Kong.

10.1021/ma071284b CCC: $40.75
Published on Web 12/29/2007

scale longer than τ_r, the chains can disentangle with each other so that the relaxation is like in a viscous liquid. On the other hand, Wang and co-workers[20−24] related the slow relaxation to the viscoelasticity under the θ condition from the osmotic pressure fluctuation without using the concept of a transient gel network. The cooperative diffusion and the viscoelastic effect are generally mixed, depending on the frequency and a coupling parameter (β). $\beta = (C/\rho)(V_S - V_P)/V_S$, proportional to the difference between partial specific volumes of polymer and solvent ($V_S - V_P$), and ρ is the solution density. The influence of longitudinal modulus on the concentration fluctuation leads to a broad distribution.[23,24] If $\beta = 1$, there exits only one stress relaxation mode. D_c becomes identical to that predicted in the transient gel network model.[4,19]

Experiments around the θ condition indicate that the solvent quality has a profound effect on the slow relaxation.[25−31] Not everyone accepts or recognizes such a slow mode, even though it has been repeatedly observed for more than three decades, because of some problems or questions related to previous light-scattering experiments, such as some earlier premature data analysis methods and the preparation of dust-free viscous semidilute solutions. As an important remaining and controversial problem in polymer science, it deserved to be reexamined; namely, (1) whether the slow mode is real, not due to some previously suggested artifacts; (2) if real, under which condition it appears; and (3) its physical nature. Advancements of laser light scattering instrumentation, including the full digital time correlator and computer, have made the dynamic study of semidilute solutions much easier and more reliable, but the preparation of dust-free viscous semidilute solutions still remains an experimental challenge.

Traditionally, viscous dust-free semidilute solutions are prepared by slow evaporation of solvent from a dust-free dilute solution (the increase of polymer concentration). On the basis of the definition of C^*, one can also change R_g or M to switch a solution from dilute to semidilute for a fixed polymer concentration. An in situ change of R_g or M or both inside a LLS cell can completely avoid possible problems of dust, solubility, and inhomogeneity. Further, a comparative study of polymer chains in an athermal solvent and in a less good solvent under an identical experimental procedure will also be very helpful. Here, we focus on the effect of solvent quality on the slow mode by using some novel solution preparation methods, different from previous studies,[17,23,32−36] including (1) using the temperature dependence of the chain conformation of polystyrene (PS) in cyclohexane to switch a solution from dilute to semidilute; and (2) using anionic living polymerization to directly prepare dust-free semidilute/concentrated solutions (up to 30%) of narrowly distributional PS chains in two different solvents. It should be noted that using the temperature, we are not only able to change C^* but also the solvent quality for PS in cyclohexane.

Experimental Section

Laser Light Scattering. A commercial LLS spectrometer (ALV/DLS/SLS-5022F) equipped with a multi-τ digital time correlation (ALV5000) and a cylindrical 22 mW UNIPHASE He−Ne laser ($\lambda_0 = 632.8$ nm) as the light source was used. The details of LLS instrumentation and theory can be found elsewhere.[37,38] In static LLS, the excess absolute time-averaged scattered light intensity, known as the excess Rayleigh ratio $R_{vv}(q)$, of a dilute polymer solution at concentration C (g/mL) is related to the weight average molar mass M_w, the root-mean square z-average radius of gyration $\langle R_g^2\rangle_z^{1/2}$ (or written as $\langle R_g\rangle$), and the scattering vector q as

$$\frac{KC}{R_{vv}(q)} \approx \frac{1}{M_w}\left(1 + \frac{1}{3}\langle R_g^2\rangle q^2\right) + 2A_2C \quad (1)$$

where $K = 4\pi^2n^2(dn/dC)^2/(N_A\lambda_0^4)$ and $q = (4\pi n/\lambda_0)\sin(\theta/2)$ with N_A, dn/dC, n, and λ_0 being Avogadro's number, the specific refractive index increment, the solvent refractive index, and the wavelength of the light in vacuum, respectively; A_2 is the second virial coefficient. The plots of $[KC/R_{vv}(q)]_{c\to 0}$ versus q^2 and $[KC/R_{vv}(q)]_{q\to 0}$ versus C, respectively, lead to $\langle R_g^2\rangle$ and A_2. In semidilute solutions, eq 1 is not applicable because molecular characteristic properties of individual chains are screened. Therefore, we have to use $\langle R_g\rangle$ and A_2 obtained in dilute solutions to estimate C^* and the segment−segment interaction.

In dynamic LLS, the intensity−intensity time auto-correlation function $G^{(2)}(q,t)$ is defined as $\langle I(q,0)I(q,t)\rangle/\langle I(q)\rangle^2$ when the homodyne mode is measured, where t is the delay time and $\langle I(q)\rangle$ is the time-average scattering intensity, i.e., the measured baseline. $G^{(2)}(q,t)$ is related to the normalized electric field−field time auto-correlation function $|g^{(1)}(t,q)|$, defined as $\langle E(0,q)E^*(t,q)\rangle/\langle E(0)E^*(0)\rangle$, by the Siegert relation as[39,40]

$$G^{(2)}(q,t) = A[1 + \beta|g^{(1)}(t,q)|^2] \quad (2)$$

where A is the measured baseline and β is the coherent factor, depending on the detection optics. For a broadly distributed relaxation, $|g^{(1)}(t,q)|$ is related to a characteristic relaxation time distribution ($G(\tau)$) as

$$|g^{(1)}(t,q)| = \int_0^\infty G(\tau)\, e^{-t/\tau}\, d\tau \quad (3)$$

The Laplace inversion of each measured $G^{(2)}(q,t)$ can lead to one $G(\tau)$ on the basis of eqs 2 and 3. In this study, the CONTIN program in the correlator was used.[41] Previously, $G^{(2)}(q,t)$ was analyzed with different methods,[16,17,23,27,42,43] including a combination of two stretched exponential functions, such as

$$[G^{(2)}(q,t) - A]/A = \beta_{apparent}\{A_f \exp[-(t/\tau_f)^{\delta_f}] + A_s \exp[-(t/\tau_s)^{\delta_s}]\}^2 \quad (4)$$

where $\beta_{apparent} \le \beta$, an apparent coherent factor; A_f and A_s are intensity contributions of the fast and slow modes, respectively; and $A_f + A_s = 1$. In this study, by varying δ_f and δ_s and comparing relative errors of different fittings, we found that one translational diffusion term (i.e., $\delta_f = 1$) plus one stretched exponential term with $0 < \delta_s < 1$ lead to the most stable results.

Sample Preparation. First, the traditional filtration was used to prepare a dilute dust-free polystyrene solution and then the solvent was gradually removed by slow evaporation. Five narrowly distributed polystyrene standards (PS1, PS2, PS3, and PS4 from Polymer Source and PS5 from Polymer Laboratories) were used as received. Both analytic grade toluene (an athermal solvent) and cyclohexane (a less good solvent in the range 34.5−50 °C and a poor solvent in the range 32−34.5 °C) were from Aldrich. Toluene was used without further purification, but cyclohexane was dehydrated under argon with sodium. The overlap concentration (C^*) for each PS sample was estimated from $3M/(4\pi N_A R_g^3)$. Molecular parameters of the PS standards in toluene are listed in Table 1. The ratio C/C^* indicates the concentration range studied. In cyclohexane, we can fix C but vary C^* by changing the solution temperature (T) in the range 33−50 °C to change R_g. All the PS solutions in toluene were clarified by 0.45 μm Millipore filters (Hydrophobic Millex-LCR, PTFE) to remove dust and then kept at 25 ± 0.1 °C for at least two weeks before LLS measurements. Dust was removed from the solutions of PS3 and PS5 in cyclohexane by a 0.45 μm Millipore filter (Hydrophobic Millex-LCR, nylon) at 50 °C. The solutions were kept at 50 °C for at least 1 month to ensure no concentration gradient inside. During the slow evaporation, a 0.1 μm filter was attached to the cell cap via a hollow needle so that no dust could enter the solution. The polymer concentration during the evaporation was determined by weight.

Table 1. Molecular Parameters of Five Polystyrene Standards in Different Solutions

sample	M_w (g/mol)	M_w/M_n	solvent	T (°C)	R_g (nm)	C^* (g/mL)	A_2 (mol cm^3/g^2)	C/C^* studied
PS1	1.16×10^5	1.06	toluene	25	13	2.2×10^{-2}	4.6×10^{-4}	1.0−4.5
PS2	5.1×10^5	1.06	toluene	25	31	6.7×10^{-3}	3.3×10^{-4}	2.6−13
PS3	1.83×10^6	1.08	cyclohexane	50	51	5.5×10^{-3}	1.7×10^{-4}	1.0−4.0
PS4	2.08×10^6	1.08	toluene	25	73	2.1×10^{-3}	2.4×10^{-4}	4.5−13
PS5	6.85×10^6	1.06	toluene	25	146	7.9×10^{-4}	1.8×10^{-4}	3.9−21
			cyclohexane	50	111	2.0×10^{-3}	3.1×10^{-5}	1.0−16

In toluene, the measurement temperature was kept at 25.0 °C. In cyclohexane, the temperature was varied in the range 33−50 °C, crossing the θ temperature (34.5 °C) without any interchain association. In each dynamic LLS measurement, the time correlation function was accumulated until the maximum difference between the measured and calculated data points was less than 0.1%. The solutions were kept at each temperature for 10 h before the LLS measurement. Even with such precaution, it is still problematic to use evaporation to prepare a concentrated solution with a higher C/C^* because it is difficult to render a large volume of dust-free dilute solution and also because the high viscosity at the later stage of evaporation hinders the removal of a possible concentration gradient. To solve this problem, we used in situ living anionic polymerization to prepare concentrated dust-free polystyrene solutions directly inside the LLS cell with a high-vacuum stopcock.

In anionic living polymerization, **s***ec*-butyllithium in *n*-hexane/cyclohexane (1.3 M) and dibutylmagnesium in heptane (1.0 M) were purchased from Aldrich. The purification methods for styrene, benzene, and cyclohexane are standard. Styrene was mixed with benzene or cyclohexane at the required volume ratio and stored at −20 °C in the refrigerator inside a drybox (MBraun Unilab, O_2 < 0.1 ppm and H_2O < 0.1 ppm) before use. The initiator solution was added into a styrene solution inside a drybox at 0 °C under stirring. The reaction mixture was immediately clarified by a 0.45 μm PTFE hydrophobic Millipore filter. The anionic living polymerization in benzene proceeded at the room temperature. In cyclohexane, the reaction was done at 45 °C for 3 days. The living chains were terminated by briefly opening the high vacuum stopcock. Each solution was kept at 50 °C for at least one week before the LLS measurement. Afterward, the degree of polymerization was determined using GPC with a Waters-1515 pump, HR3, HR4, and HR6 Waters-Styragel columns, and a Wyatt MALLS detector. THF was used as the eluent in GPC, and the flow rate was 1 mL/min.

Results and Discussion

In a creditable and reliable LLS experiment, the preparation of a dust-free solution is vitally important, especially for viscous semidilute solutions. To verify whether the previously observed slow mode is due to some artifacts, we first repeated studies of polystyrene (PS) in toluene.[7,17,32] We first clarified a dilute solution by filtration. The solution temperature was kept at 25 °C to allow a gradual removal of solvent so that the solution changed from dilute to semidilute. In our experiments, the evaporation was so slow that the whole process lasted for about 1 year from the initial dilute solution to the final highest concentration. In this way, the chains have sufficient time to diffuse so that a possible concentration gradient inside the solution, especially at the later stage of evaporation, can be avoided.

Figure 1 shows how the polymer concentration (C) increases with the evaporation time (t). The inset shows that the time-average excess scattering intensity ($\langle I\rangle_{q\to 0} = \langle I\rangle_{\text{solution}} - \langle I\rangle_{\text{solvent}}$) decreases as C increases, following a scaling of $\langle I\rangle_{q\to 0} \propto C^{-0.25\pm0.05}$. For a polymer solution,[2] $\langle I\rangle_{q\to 0} \propto (k_BT/V)C/(\partial\pi/\partial C)$, where $\partial\pi/\partial C$ is the osmotic compressibility. In dilute solutions, $\partial\pi/\partial C = N_Ak_BT/M$ and then $\langle I\rangle_{q\to 0} \propto C$. In semidilute solutions, $\partial\pi/\partial C \propto C^{5/4}$ so that $\langle I\rangle_{q\to 0} \propto C^{-1/4}$. Such a scaling can also be discussed from another perspective as follows. Assuming that each chain in a semidilute solution can be divided into a number of subchains or segments ("blobs") and all the "blobs" are independent, we have $\langle I\rangle_{q\to 0} \propto N_{\text{blob}}(n_{\text{blob}})$,[2] where N_{blob} and n_{blob} are the numbers of blobs in a semidilute solution and monomer units inside each blob, respectively. Note that $N_{\text{blob}}n_{\text{blob}}$ is the total number of segments (N_{segment}) and proportional to C. On the other hand, the correlation length (ξ) is related to C as $\xi \propto C^{-0.75}$ and $\xi \propto n_{\text{blob}}^{0.6}$ in an athermal solvent since each segment inside a blob is still a self-avoiding Gaussian chain. Therefore, we also obtain $\langle I\rangle_{q\to 0} \propto C^{-0.25}$. The scaling in the inset agrees well with the prediction and shows that the solutions studied are indeed in the semidilute regime.

As expected,[4,6] only one fast relaxation mode is observed over the entire concentration range, consistent with some of the previous studies.[1,5] Its related average line-width ($\langle\Gamma\rangle_f = 1/\langle\tau\rangle_f$) is not only a linear function of q^2 but also passing through the origin as $q \to 0$, a characteristic of diffusive relaxation. The slope of $\langle\Gamma\rangle_f$ versus q^2 leads to a cooperative diffusion coefficient (D_C), or further, to the dynamic correlation length (ξ_D) defined by the Stokes−Einstein equation, $\xi_D = k_BT/6\pi\eta_0D_C$. On the other hand, we can also get the static correlation length (ξ_S) of a semidilute solution from the angular dependence of $\langle I(q)\rangle$ using the Ornstein−Zernike equation.[8,43,46] Both $\xi_{D,\text{fast}}$ and $\xi_{S,\text{fast}}$ are scaled to C as $\xi_{\text{fast}} \sim C^{-0.72\pm0.02}$, similar to previous results.[1,9,10]

In an athermal solvent, linear polymer chains in a semidilute solution entangle with each other to form a transient network and the solvent−segment interaction is stronger than the segment−segment interaction. Therefore, thermally agitated motions of the segments inside different blobs are independent from each other and the light scattered from them is not correlated. In other words, *each chain is confined inside a uniform tube and all the blobs are dynamically "identical"*. The intensity−intensity time correlation function only reflects diffusive motions of the segments inside each blob, arrested around their gravity center in a short time scale. In a parallel experiment, using the same solution-preparation method, we further studied dynamics of semidilute solutions of polystyrene in cyclohexane, a less good solvent even at 50 °C.

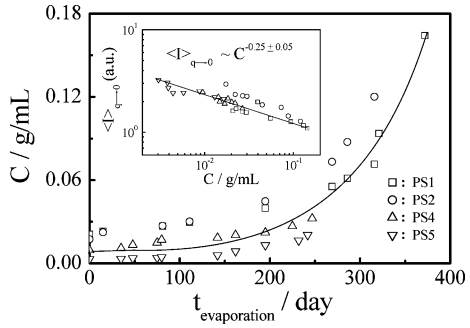

Figure 1. Evaporation time dependence of concentration (C) of four polystyrene standards (PS1, PS2, PS4, and PS5) in toluene. The inset shows concentration dependence of average scattering intensity ($\langle I\rangle_{q\to 0}$) as scattering vector ($q$) approaches zero.

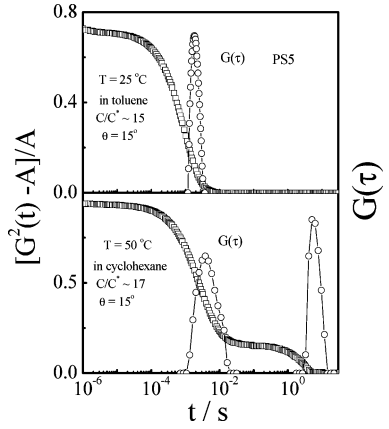

Figure 2. Intensity−intensity time correlation functions and characteristic relaxation time distributions ($G(\tau)$) of PS5 in toluene (an athermal solvent at 25 °C) and in cyclohexane (a good solvent at 50 °C) with a similar reduced concentration.

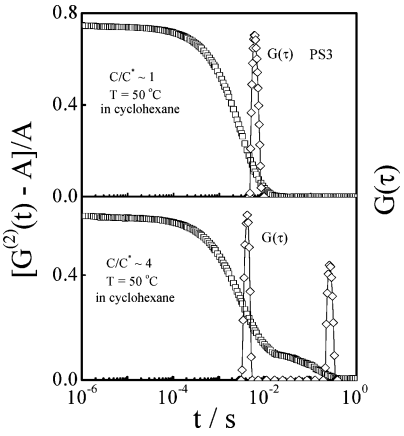

Figure 3. Intensity−intensity time correlation functions and characteristic relaxation time distributions ($G(\tau)$) of PS3 in cyclohexane in two different concentration regimes; namely, dilute ($C/C^* \sim 1$) and semidilute ($C/C^* \sim 4$).

Figure 2 shows a comparison of dynamics LLS results in toluene and in cyclohexane. The results were different even though the solutions were prepared by an identical procedure. There is an additional slow mode in cyclohexane with a similar reduced concentration (C/C^*). Moreover, Figure 3 shows that such a slow relaxation mode in cyclohexane appears only when $C > C^*$. Note that cyclohexane at 50 °C is not an athermal solvent for polystyrene because the θ-temperature (T_Θ) is ~34.5 °C. The slight shift of the fast mode to the left (even faster) as C increases is reasonable and expected because its related dynamic correlation length (ξ_{blob}) decreases as C increases. Because of a similar reason, the intercept at $t \rightarrow 0$, i.e., β_{app}, also becomes smaller in the semidilute solution because $\langle I \rangle_{blob}$ decreases with ξ_{blob}.

To ensure that such prepared semidilute solutions are free from dust particles or insoluble chain aggregates or a possible concentration gradient, we measured the sample position dependence of time-average scattering intensities $\langle I \rangle$ by randomly lifting and rotating the scattering cell to let the incident laser beam hit different parts of the solution. $\langle I \rangle$ randomly fluctuates around an average value and no speckle so that the solution is "homogeneous". Note that the scattering volume is about 200 × 200 × 200 μm^3 at 90°. Further, we monitored $\langle I \rangle_{q \rightarrow 0}$ during one cooling-and-heating cycle. We found a sharp increase of $\langle I \rangle_{q \rightarrow 0}$ at ~33 °C, signaling interchain aggregation. In the temperature range 34−55 °C, the solution is in a one-phase region. Hereafter, we only vary the temperature in this range to avoid phase separation. The reversible temperature dependence of $\langle I \rangle_{q \rightarrow 0}$ without any hysteresis further shows that the observed slow mode in the solution is not due to some suggested artifacts.[16,17,23,27,47−49]

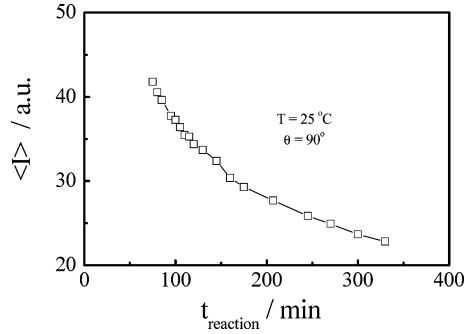

Figure 4. Reaction-time dependence of time-average scattering intensity ($\langle I \rangle$) during in situ anionic polymerization of styrene in benzene inside a light-scattering cell.

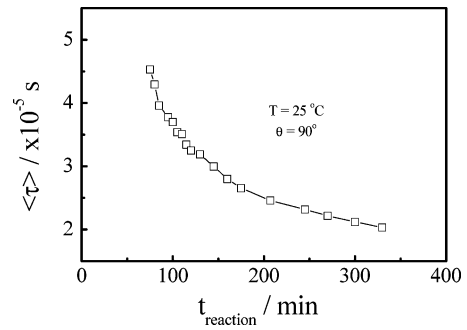

Figure 5. Reaction time dependence of average characteristic relaxation time ($\langle \tau \rangle$) during in situ anionic polymerization of styrene in benzene inside a light-scattering cell.

In the above parallel and comparative studies, we only change an athermal solvent (toluene) to a less good solvent (cyclohexane). To further prove that the slow mode observed for polystyrene in cyclohexane in the temperature range 34−55 °C is real, we decided to use living anionic polymerization to prepare more concentrated dust-free solutions directly inside the LLS cell with a high vacuum stopcock, starting from a dust-free monomer solution. Initially, we tried to follow the kinetics of the polymerization of styrene in benzene using an in situ LLS measurement but failed because the initial reaction was too fast to be measured. Only at the later stage, can we change the time-average scattering intensity $\langle I \rangle_{q \rightarrow 0}$ and measure the time correlation function to obtain the characteristic relaxation time ($\langle \tau \rangle$).

Figures 4 and 5 show the reaction time dependence of $\langle \tau \rangle$ and $\langle I \rangle_{q \rightarrow 0}$. A combination of the scaling laws, $\xi_{blob} \propto \tau \propto C^{-\mu}$ and $\langle I \rangle_{blob} \propto N_{blob}(n_{blob})^2 \propto n_{blob} C \propto \xi_{blob}{}^{1/\nu} C$ should lead to $\langle I \rangle \propto \tau^{(1/\nu - 1/\mu)}$, where $\mu = 0.75$ and $\nu = 0.6$ in an athermal solvent. Assuming a constant viscosity, we would have $\langle I \rangle \propto \tau^{1/3}$. However, Figure 6 shows that $\langle I \rangle \propto \langle \tau \rangle^{0.77}$. The scaling exponent is much larger than $^1/_3$. Note that the data points are slightly curved and the slope decreases as $\langle \tau \rangle$ increases. The high exponent indirectly suggests that the microviscosity is not a constant during the polymerization.[28,65] At the end of polymerization of each solution, we can terminate living PS chains and measure their weight average molar mass (M_w). For the solution studied in Figures 4−6, we found that $M_w \sim 5.3 \times 10^5$ g/mol and the polymer concentration is 0.18 g/mL, i.e., $C/C^* \sim 30$. Even with such a high concentration, there is still only one fast relaxation mode, agreeing well with the prediction in an athermal solvent.

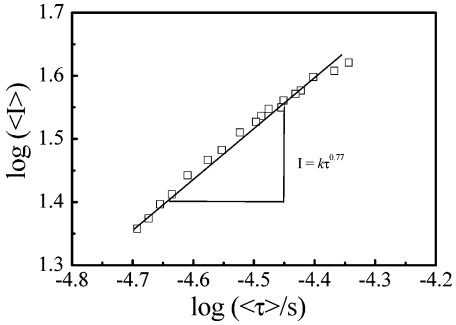

Figure 6. Scaling between time-average scattering intensity $\langle I \rangle$ and average characteristic relaxation time $\langle \tau \rangle$ during in situ anionic polymerization inside a LLS cell.

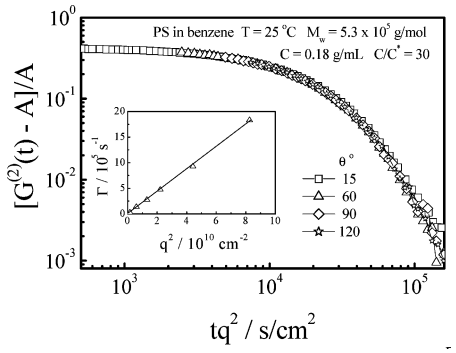

Figure 7. Scattering vector dependence of intensity−intensity time correlation functions of polystyrene in benzene, where the delay time (t) is scaled with q^2. The inset shows scattering vector dependence of the average line-width.

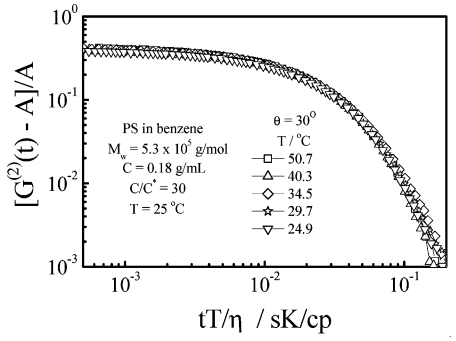

Figure 8. Temperature dependence of intensity−intensity time correlation functions of polystyrene in benzene, where delay time (t) is scaled with solution temperature (T) and solvent viscosity (η).

As shown in Figure 7, the scaling of the delay time (t) with q^2 makes the measured time correlation functions at different scattering angles collapse into one curve. The inset shows that the average line-width ($\langle \Gamma \rangle_f = 1/\langle \tau \rangle_f$) is a linear function of q^2, passing through the origin, a characteristic of diffusive relaxation. As discussed before, this fast relaxation mode could be modeled as the cooperative motions of the "blobs" confined inside a "tube" made of its surrounding chains. Using the identical anionic polymerization procedure, we prepared three additional solutions of polystyrene in benzene ($M_w = 4.83 \times 10^4$ g/mol, $M_w/M_n = 1.05$, and $C = 0.091$ g/mL; $M_w = 1.14 \times 10^5$ g/mol, $M_w/M_n = 1.07$, and $C = 0.11$ g/mL; $M_w = 2.86 \times 10^4$ g/mol, $M_w/M_n = 1.17$, and $C = 0.18$ g/mL). Only one fast relaxation mode was observed in their measured intensity−intensity time correlation functions. Figure 8 shows that such a fast relaxation mode is also independent of the solution temperature (T) after the scaling of the delay time (t) with T and the solvent viscosity, which is expected because benzene is an athermal solvent for PS in the temperature range studied.

Some previous studies of linear homopolymer chains in an athermal solvent also showed an additional slow relaxation mode.[7,16,32,44,45] In comparison with the current results, those observed slow modes could only be attributed to artifacts, such as a concentration gradient, imperfect dissolution, polydispersity, or dust particles. The earlier attribution of such a slow mode to the chain reptation is certainly incorrect because dynamic LLS cannot distinguish one chain from surrounding chains in a homopolymer solution,[2,6] except for a polymer sample with a high polydispersity. After showing that the slow relaxation mode is real and only appears when the solvent quality is less good, we hereafter only discuss the results of PS in cyclohexane. Table 2 summarizes parameters of 10 solutions of PS in cyclohexane with different concentrations and average molar masses prepared by living anionic polymerization.

Figure 9 shows that there is only one expected fast relaxation mode in cyclohexane when the solution is dilute, independent of the scattering angle. As soon as the solution becomes semidilute, i.e., $C/C^* > 1$, an additional slow relaxation mode appears in the measured intensity−intensity time correlation function. The analysis of such a time correlation function on the basis of eq 4 leads to two characteristic relaxation times ($\langle \tau \rangle_f$ and $\langle \tau \rangle_s$). Figure 10 shows that for Solution 1 listed in Table 2, the slow mode becomes more obvious at smaller scattering angles. Note that in LLS, the observation length is directly proportional to $1/q$, i.e., large objects are more visible at smaller scattering angles. Also note that here C/C^* is only ~1.4 at 45 °C and $C/C_e \sim 0.1$ so that most of the chains are not entangled with each other. In a less good solvent, those entangled chains behave like large transient clusters within the delay time window in dynamic LLS due to relatively stronger segment−segment interaction in comparison with in an athermal solvent. Moreover, we found that the characteristic line-width ($\langle \Gamma_s \rangle$) is scaled to q as $\langle \Gamma_s \rangle \sim q^3$, also indicating that the slow mode reflects some internal motions of large scattering objects. We will come back to this point later.

On the other hand, Figures 11 and 12 reveal that at a low scattering angle, the decrease of the solution temperature makes the slow mode less obvious and results in a decrease of its intensity contribution (the peak area). At 37 °C, the slow mode completely disappears in the whole angular range and only one fast mode is observable. For Solutions 2 and 3 listed in Table 2, we get a similar result. As discussed before, the decrease of the solution temperature makes the solvent quality poorer and the segment−segment interaction stronger so that polystyrene chains contract as the temperature decreases, resulting in an increase of C^*, which can switch a solution from semidilute to dilute for a given C, i.e., from $C/C^* > 1$ to $C/C^* < 1$ when C/C^* is not higher at higher temperatures. *Our comparative studies of different solvents, concentrations, and temperatures convincingly demonstrate that the slow mode is real due to the solvent quality, not due to some previously suggested artifacts.* Note that using the temperature, we only change C^* in a limited range. For a more concentrated polystyrene solution, the decrease of the solution temperature cannot switch it from semidilute to dilute.

Figure 13 shows that for a more concentrated solution, the decrease of the solution temperature leads to the increase of the intensity contribution of the slow mode. Here, the double logarithmic plot makes the slow mode more visible in the measured time correlation functions, but its actual intensity contribution is only a few percent, which can be better viewed in its related peak area (A_s) in the characteristic relaxation time distribution $G(\tau)$ calculated from the Laplace inversion of the

Table 2. Characterization of Solutions of Polystyrene in Cyclohexane Prepared by Living Anionic Polymerization Directly Inside a Laser Light-Scattering Cell

solution	C (g/mL)	M_w (g/mol)	M_w/M_n	C^* (g/mL)	$C/C^*_{45\ °C}$	C_e (g/mL)[a]	C/C_e
1	9.1×10^{-2}	4.6×10^4	1.07	6.5×10^{-2}	1.4	7.8×10^{-1}	0.1
2	1.1×10^{-1}	9.7×10^4	1.07	3.9×10^{-2}	2.8	3.7×10^{-1}	0.3
3	1.8×10^{-1}	5.8×10^4	1.06	5.6×10^{-2}	3.2	6.2×10^{-1}	0.3
4	1.8×10^{-1}	1.1×10^5	1.06	3.5×10^{-2}	5.1	3.3×10^{-1}	0.6
5	1.8×10^{-1}	1.7×10^5	1.20	2.5×10^{-2}	7.1	2.1×10^{-1}	0.9
6	1.4×10^{-1}	5.5×10^5	1.08	1.2×10^{-2}	12	6.5×10^{-2}	2.2
7	1.8×10^{-1}	4.8×10^5	1.09	1.1×10^{-2}	16	7.5×10^{-2}	2.4
8	2.7×10^{-1}	5.4×10^5	1.08	1.1×10^{-2}	25	6.7×10^{-2}	4.0
9	1.8×10^{-1}	1.4×10^6	1.15	5.1×10^{-3}	35	2.6×10^{-2}	6.9
10	2.2×10^{-1}	1.9×10^6	1.13	4.3×10^{-3}	51	1.9×10^{-2}	12.0

[a] Where C_e is defined as M_e/M_w with $M_e = 3.6 \times 10^4$ g/mL (ref 48).

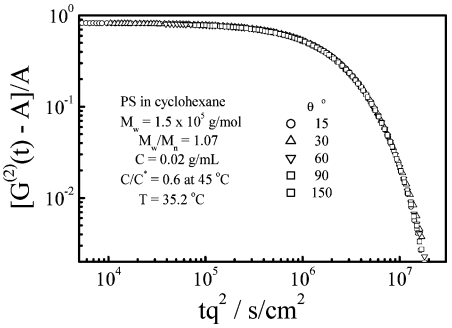

Figure 9. Scattering vector dependence of intensity−intensity time correlation functions of polystyrene in cyclohexane, where the delay time (t) is scaled with q^2.

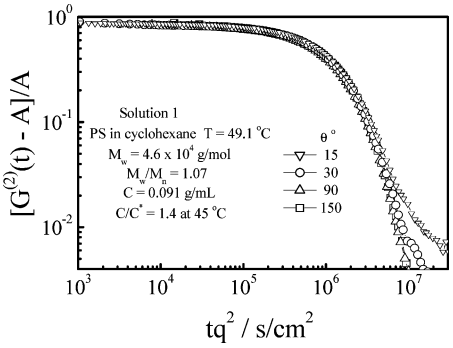

Figure 10. Scattering vector dependence of intensity−intensity time correlation functions of polystyrene in cyclohexane (Solution 1), where the delay time (t) is scaled with q^2.

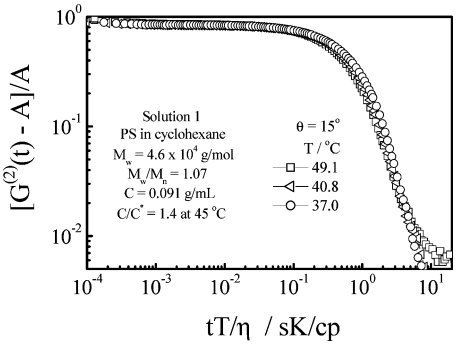

Figure 11. Temperature dependence of intensity−intensity time correlation functions of polystyrene in cyclohexane (Solution 1), where the delay time (t) is scaled with solution temperature (T) and solvent viscosity (η).

measured time correlation function, as shown in Figure 14. The peak area (A_s) increases from ~5% to ~9% as the temperature decreases from 50 °C to 34 °C (a poor solvent). When $C/C^* > 5$ or more precisely $C/C_e > 1$, all the chains are entangled with each other and the solution contains one transient polymer

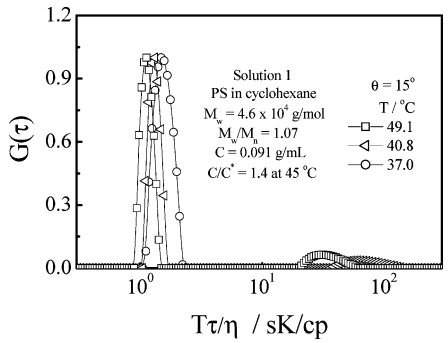

Figure 12. Temperature dependence of the characteristic relaxation time distributions $G(\tau)$ of polystyrene in cyclohexane (Solution 1), where the characteristic relaxation time (τ) is scaled with solution temperature (T) and solvent viscosity (η).

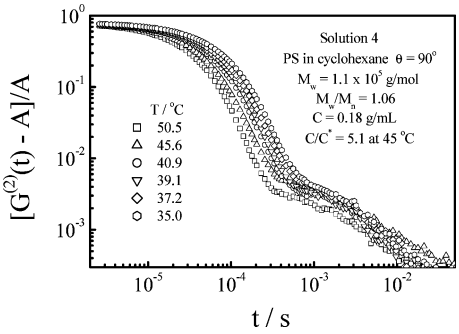

Figure 13. Temperature dependence of intensity−intensity time correlation functions of polystyrene in cyclohexane (Solution 4).

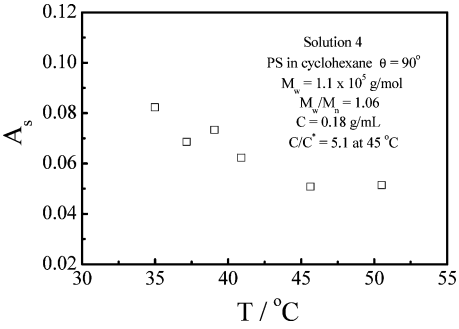

Figure 14. Temperature dependence of the scattering-intensity contribution of the slow mode, where each A_s, the peak area of the slow mode in ($G(\Gamma)$), is calculated from one corresponding $[G^{(2)}(t) - A]/A$ in Figure 13 on the basis of eqs 2−4.

"cluster". In a short time scale, each chain is arrested around its center of gravity and only its segments (blobs) can jiggle around inside the "tube".

Figure 15 shows that the fast mode is collapsed together when the decay time (t) is scaled by q^2, revealing its diffusive nature. In contrast with Figure 10, *here the slow mode becomes more*

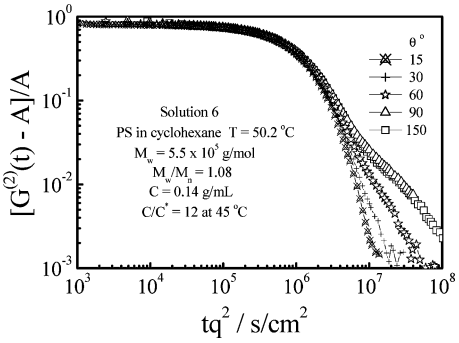

Figure 15. Scattering vector dependence of intensity−intensity time correlation functions of polystyrene in cyclohexane (Solution 6), where delay time (t) is scaled with q^2.

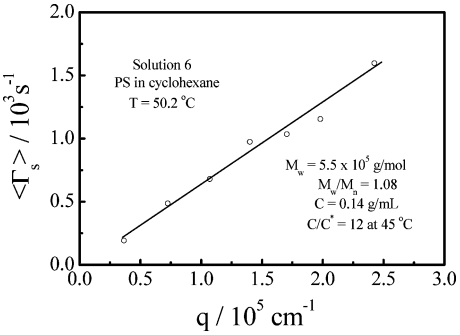

Figure 16. Scattering vector dependence of the average characteristic line-width ($\langle\Gamma\rangle_s$) of the slow mode from corresponding $[G^{(2)}(t) - A]/A$ in Figure 15 on the basis of eqs 2−4.

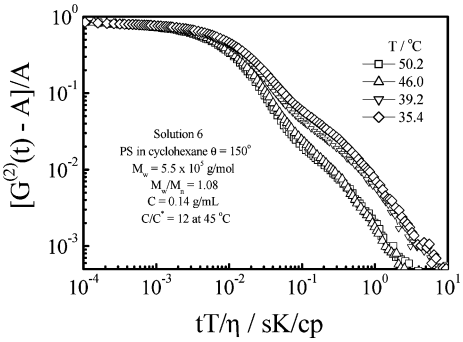

Figure 17. Temperature dependence of intensity−intensity time correlation functions of polystyrene in cyclohexane (Solution 6), where the delay time (t) is scaled with solution temperature (T) and solvent viscosity (η).

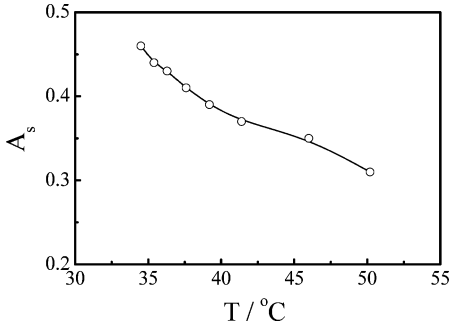

Figure 18. Temperature dependence of the scattering-intensity contribution of the slow mode, where each A_s, the peak area of the slow mode in ($G(\Gamma)$), is calculated from one corresponding $[G^{(2)}(t) - A]/A$ in Figure 17 on the basis of eqs 2−4.

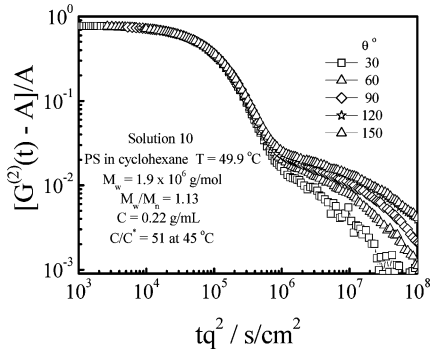

Figure 19. Scattering vector dependence of intensity−intensity time correlation functions of polystyrene in cyclohexane (Solution 10), where the delay time (t) is scaled with q^2.

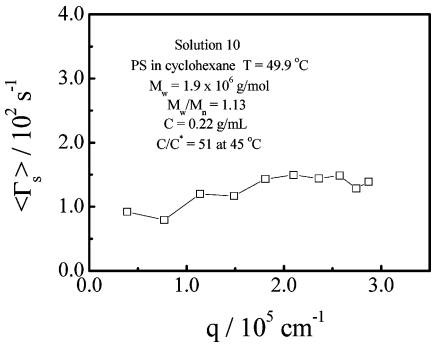

Figure 20. Scattering vector dependence of the average characteristic line-width ($\langle\Gamma\rangle_s$) of the slow mode from corresponding $[G^{(2)}(t) - A]/A$ in Figure 19 on the basis of eqs 2−4.

obvious at larger scattering angles, which is different from those observed in the above lower concentration region. It implies that the slow mode is not related to some large scattering objects. Figure 16 shows that its characteristic line-width ($\langle\Gamma\rangle_s$) is proportional to the scattering vector (q). We will come back to discuss the concentration dependence of the scaling exponent (α_s) between $\langle\Gamma\rangle_s$ and q. Moreover, Figures 17 and 18 reveal that as the solution temperature decreases, the slow mode becomes slower and its intensity contribution (A_s) increases for a given scattering angle. Note that cyclohexane at 50 °C is a good, but not athermal, solvent for polystyrene.

Further increase of the polymer concentration makes the slow mode even visible at low scattering angles, as shown in Figure 19. Here, $C/C^* > 50$ and the solution appears like a gel without any visible flow within a short time, but the solution is homogeneous and its scattering intensity is independent of the position of the scattering volume inside the solution. Figure 19 clearly shows that the fast mode collapsse together after the delay time (t) is scaled by q^2, indicating that it remains diffusive. At the same time, Figure 20 shows that $\langle\Gamma\rangle_s$ is nearly independent of q and remains finite even at $q \rightarrow 0$. Once again, Figure 21 shows that for a given scattering angle, the slow mode becomes slower and its intensity contribution (A_s) increases as the solution temperature decreases, presumably due to stronger segment−segment interaction. Note that here we have scaled the delay time (t) with the solution temperature and solvent viscosity so that $G^{(2)}(q,t)$ at different temperatures can be directly compared.

Figure 22 summarizes the concentration dependence of the scaling exponents (α_f and α_s) in $\langle\Gamma\rangle_f \propto q^{\alpha_f}$ and $\langle\Gamma\rangle_s \propto q^{\alpha_s}$. As expected, for the fast mode, $\langle\Gamma\rangle_f \propto q^2$ over the entire concentration range studied, reflecting the diffusive Brownian motion of the gravity center of each segment (blob). In contrast, for the slow mode, α_s decreases as C/C_e increases. We can roughly divide Figure 22 into two concentration regions (left and right) using $\alpha_s = 2$ as a reference (the dashed line). On the left (C/C_e

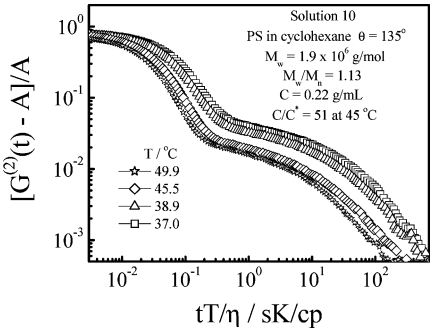

Figure 21. Temperature dependence of intensity−intensity time correlation functions of polystyrene in cyclohexane (Solution 10), where the delay time (t) is scaled with solution temperature (T) and solvent viscosity (η).

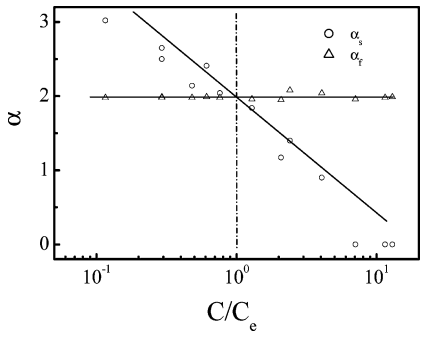

Figure 22. Polymer concentration dependence of two scaling exponents (α_f and α_s) in $\langle\Gamma\rangle_f \propto q^{\alpha_f}$ and $\langle\Gamma\rangle_s \propto q^{\alpha_s}$ for polystyrene in cyclohexane (a good solvent at 45 °C).

$< \sim 1$), the slow mode is more visible at smaller scattering angles, but in the right region ($C/C_e > 1$), its intensity contribution to $G(\tau)$ increases with the scattering angle. As mentioned before, the LLS theory tells us that larger objects scatter more light at a lower scattering angle. Therefore, in the left region, the slow mode should be related to scattering objects larger or comparable with $1/q$; while in the right region, it is related to scattering objects smaller than $1/q$. The LLS theory also tells us that when the scaling exponent (α) between the characteristic line-width ($\langle\Gamma\rangle$) and the scattering vector (q) is larger than 2, we are observing a mixture of diffusion and internal motions of larger scattering objects. However, it is not clear why α is smaller than 2 in a three-dimensional space. Next, we will discuss and speculate the nature of this additional slow mode.

Using the relaxation gel model, Doi and Onuki[64] showed that the osmotic modulus is much higher than the shear modulus in a good solvent, but they are comparable in the θ solvent. This is why there is only one fast relaxation mode in semidilute solutions if the solvent is athermal, but an additional slow relaxation mode appears in the θ solvent. Later, Wang et al.[23] studied semidilute solutions using the modified hydrodynamic equation. They found that the osmotic modulus is lower than the shear modulus, independent of the solvent quality. The literature values of α_s range from 4 to 0 for different polymer solutions and melts.[50−58] Our current study shows a systematic change of α_s for one well-defined polymer/solvent system over a wide polymer concentration range ($1 \leq C/C^* \leq 51$).

When the existence of the slow mode in a less good solvent becomes irrefutable, one can still argue that it is due to the slow density fluctuation induced by the relaxation of the "tube", i.e., it is indirectly related to the reptation. Similarly, inside a concentrated colloidal dispersion, dynamic LLS studies reveal two relaxation modes at higher scattering angles. It has been

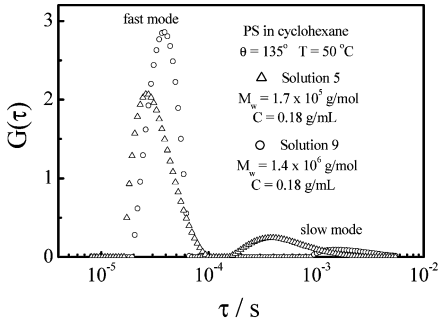

Figure 23. Characteristic relaxation time distributions of Solutions 5 and 9. Note that all the conditions are the same, except chain length in Solution 9 is ~10 times longer.

attributed to the rattling of individual particles in the cage made of its surrounding particles and the slower restructuring of the cages. Here, the relaxation of the "tube" is similar to the relaxation of the cage. To test such a possibility, we studied the chain-length dependence of the slow mode. Solutions 5 and 9 listed in Table 2 have similar polymer concentrations, but the chains in Solution 9 are ~10 times longer than those in Solution 5. Their reptation times should be different by $\sim 10^3$ times. Therefore, the relaxation of the "tube" in Solution 9 should be much slower. However, Figure 23 shows that the chain length has a much smaller effect on the average characteristic relaxation time ($\langle\tau\rangle_s \sim 10^{-3}$ s) of the slow mode (the peak position). Note that the correlator can cover up to 100 s in its delay time. Therefore, the relaxation at $\langle\tau\rangle_s \sim 1$ s can easily be measured. It clearly indicates that the slow mode is not related to the chain reptation or the relaxation of the "tube".

The two relaxation modes suggest that these macroscopically homogeneous solutions must be microscopically inhomogeneous, at least, within the typical delay time window (<1 s) used in the time correlator. There are two different possibilities; namely, the coexistence of scattering objects with two different sizes in one microenvironment or similar scattering objects relax in two different microenvironments. Recently, theoretical studies and computer simulations of polymer solutions or mixtures on some noncovalent monomer−monomer interaction confirm that sufficiently strong interaction can affect the chain dynamics.[59−63] Adam et al.[25] found that in a good solvent, microscopic and macroscopic viscosities are similar, but in a less good solvent, microscopic viscosity varies with the coupling between solvent and polymer relaxation times, strongly depending on the temperature as well as the nature of solvent and polymer. In an athermal solvent, the segment−segment interaction is completely shielded by the solvent−segment interaction, so that each blob moves independently and experiences a similar microenvironment. In a less good solvent, one has to consider the segment−segment interaction.

Previously, we speculated that the slow mode might be related to some long-range density fluctuation.[9,43] Our current results indicate that for $C/C_e < \sim 1$, the slow mode is related to some large structures (scattering objects or long-range density fluctuation) since it is more visible at lower scattering angles and the scaling exponent (α_s) is higher than 2. Such large structures could be attributed to a few transient clusters made of lightly entangled chains due to relatively stronger segment−segment interaction in a less good solvent. In this case, most of the chains are not entangled with each other and they coexist with those transient "clusters", as schematically shown in Figure 24A. Strictly speaking, these solutions are not semidilute but a transitional region between dilute and semidilute solutions. Our

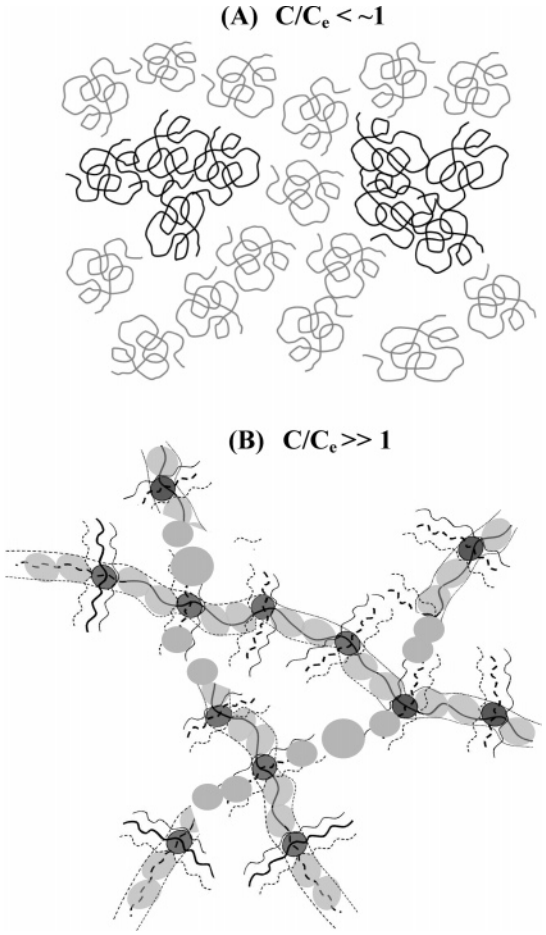

Figure 24. Schematic of semidilute polymer solutions in a less good solvent in different concentration regions: (A) $C/C_e < \sim 1$, where individual chains and "clusters" have the same microenvironment but different sizes and (B) $C/C_e > 1$, where the blobs have a similar size but different microenvironments.

results reveal that one should use C_e instead of C^* to mark the real boundary of semidilute solutions. In the transitional region ($C^* \leq C \leq C_e$), it is these transient chain entanglements that make the solution microscopically inhomogeneous over a short time scale ($\sim 10^{-3}$ s).

When $C > C_e$, all the chains inside the solution entangle with each other to form one huge "cluster". Each chain could be visualized to arrest inside a "tube" made of its surrounding chains within a short time and "divided" into a number of segments (blobs) with a dimension limited by the tube diameter (the correlation length). Within each blob, the segment is excited by thermal energy (k_BT) so that its center of gravity undergoes a Brownian motion. These thermal blobs have a similar size. In an athermal solvent, there is no interaction between them and the tube so that they experience a similar microenvironment, resulting in only one (fast) relaxation mode. In a less good or θ solvent, the segment−segment interaction near the entanglement points is expected to be stronger. Therefore, the blobs near each entanglement point should move slower than those in the middle between two entanglement points; namely, the blobs experience two different microenvironments, as schematically shown in Figure 24B. The increase of polymer concentration makes the tube thinner. Up to one point, the motions of the segments perpendicular to the tube near the entanglement point is so limited that the segments can only randomly oscillate in the tube. This might explain why its characteristic relaxation time becomes less dependent on or even independent of the scattering vector.

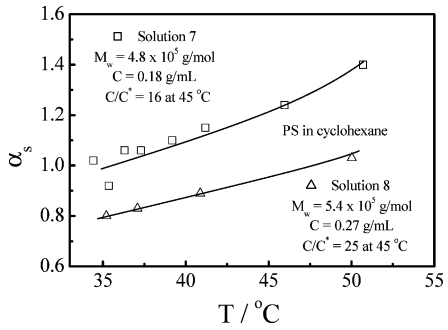

Figure 25. Temperature dependence of scaling exponent of the slow mode $(\alpha_s)\langle\Gamma\rangle_s \propto q^{\alpha_s}$ for polystyrene in cyclohexane (a good solvent at 45 °C).

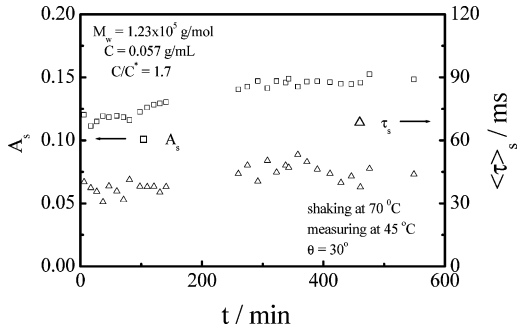

Figure 26. Time dependence of the scattering-intensity contribution (A_s) and average characteristic relaxation time $\langle\tau_s\rangle$ of the slow mode for one solution of polystyrene in cyclohexane after it is shaken at 70 °C.

The temperature dependence of both $\langle\tau\rangle_s$ and A_s supports our speculation about the nature of the slow mode. The decrease of the solution temperature makes the segment−segment interaction stronger so that each chain contracts. Note that when $C/C_e < 1$, in the left region of Figure 22, the decrease of the solution temperature has two opposite effects on the slow mode. On the one hand, it increases the segment−segment interaction and enhances the slow mode; on the other hand, the chain contraction disentangles the transient clusters. When the latter is dominant, the slow mode becomes weak or even disappears at lower solution temperatures. When $C > C_e$, the chain contraction cannot switch the solution from semidilute to dilute so that decreasing the solution temperature only increases the segment−segment interaction. This is why the slow mode becomes slower and more visible at lower temperatures. Figure 25 shows that α_s decreases with the solution temperature.

To test the coexistence of individual chains and large transient chain clusters in the region of $C/C_e < 1$, we heated one solution to 70 °C and shook it. The idea is as follows. If the solution contains some large transient clusters, the shaking may disintegrate some of them. If the clustering is a slow diffusion-controlled process, we may catch it by static and dynamic LLS. As shown in Figure 26, both A_s and $\langle\tau_s\rangle$ slowly increase with time over a period of ~10 h after the shaking. It is helpful to state that the overall scattering intensity from static LLS also slowly increases over the same time period (not shown). The shaking experiments indeed reveal that the solution contains a small number of weakly associated transient clusters. At this moment, we have no explanation why the clustering is so slow.

Conclusion

Using in situ anionic polymerization to directly prepare macroscopically homogeneous dust-free semidilute/concentration polystyrene (PS) solutions inside a laser light-scattering

(LLS) cell, we comparatively reexamined solution dynamics of PS in an athermal solvent (toluene) and in a less good/θ solvent (cyclohexane in the range 34−50 °C) by a combination of static and dynamic LLS. We confirm that in toluene there is only one fast diffusive relaxation mode in the measured intensity−intensity time correlation function even for the solution with a concentration (C) 30 times higher than the overlapping concentration (C^*). In cyclohexane, an additional slow mode appears as soon as $C/C^* > 1$. Our results show that the slow mode is real, not due to previously suggested artifacts in the solution preparation. The concentration, temperature, and time dependence of the characteristic relaxation time of the slow mode ($\langle\tau\rangle_s$), the scaling exponent (α_s) between $\langle\tau\rangle_s$ and the scattering vector (q), and the relative intensity contribution (A_s) of the slow mode suggests that such a slow mode has two different natures, depending on the polymer concentration.

When C is higher than the overlapping concentration (C^*) but lower than the entanglement concentration (C_e), only some of the chains are entangled together to form large transient clusters which coexist with individual (nonentangled) chains in the solution. In such a transitional region between dilute and semidilute solutions, the relatively stronger segment−segment interaction in a less good/θ solvent makes the movements of the chains inside each cluster more correlated within a short delay time window (<1 s) and leads to the slow mode. When $C > C_e$, all the chains are entangled with each other to form one huge "cluster". Each chain is confined inside a "tube" made of its surrounding chains and the gravity center of each chain segment (blob) fluctuates inside the tube within a short time scale ($\sim 10^{-3}$ s). In an athermal solvent, there is no interaction among the chains so that all the blobs are in the same microenvironment, leading to only one fast relaxation mode. In a less good/θ solvent, the relatively stronger segment−segment interaction near the entanglement points makes the tube nonuniform. It can be visualized that each chain is inside a nonuniform tube with a bandlike structure. Therefore, the blobs experience two different microenvironments. The restricted movement of the blobs near the entanglement points results in the slow mode.

Acknowledgment. The financial support of the Chinese Academy of Sciences (CAS) Special Grant (Grant KJCX2-SW-H14), the National Natural Scientific Foundation of China (NNSFC) Projects (Projects 20534020 and 20574065), and the Hong Kong Special Administration Region (HKSAR) Earmarked Project (Project CUHK4025/04P, 2160242) is gratefully acknowledged.

References and Notes

(1) Brown, W.; Nicolai, T. *Colloid Polym. Sci.* **1990**, *268*, 977.
(2) Teraoka, I. *Polymer Solution*; John Wiley & Sons, Inc: New York, 2002.
(3) Takahashi, Y.; Noda, I.; Nagasawa, M. *Macromolecules* **1985**, *18*, 2220.
(4) De Gennes, P. G. *Macromolecules* **1976**, *9*, 587. De Gennes, P. G. *Macromolecules* **1976**, *9*, 594.
(5) Daoud, M.; Cotton, J. P.; Farnoux, B.; Jannink, G.; Sarma, G.; Benoit, H.; Duplessix, R.; Picot, C.; De Gennes, P. G. *Macromolecules* **1975**, *8*, 804.
(6) De Gennes, P. G. *Scaling Concepts in Polymer Physics*; Cornell University Press: Ithaca, NY, 1979.
(7) Koike, A.; Nemoto, N.; Inoue, T.; Osaki, K. *Macromolecules* **1995**, *28*, 2339.
(8) Tao, H.; Huang, C.; Lodge, T. P. *Macromolecules* **1999**, *32*, 1212.
(9) Ngai, T.; Wu, C. *Macromolecules* **2003**, *36*, 848.
(10) Chu, B.; Nose, T. *Macromolecules* **1980**, *13*, 122.
(11) Ewen, B.; Richter, D.; Farago, B.; Stühn, B. *J. Non-Cryst. Solids* **1994**, *172−174*, 1023.
(12) Rital, A.; Belkoura, L.; Woermann, D. *Phys. Chem. Chem. Phys.* **1999**, *1*, 1947.
(13) Wiltzius, P.; Hans, H. R.; Cannell, D. S.; Schaefer, D. W. *Phys. Rev. Lett.* **1983**, *51*, 1183.
(14) Amis, E. J.; Han, C. C. *Polymer* **1982**, *23*, 1403.
(15) Melnichenko, Y. B.; Brown, W.; Rangelov, S.; Wignall, G. D.; Stamm, M. *Phys. Lett. A* **2000**, *268*, 186.
(16) Adam, M.; Delsanti, M. *Macromolecules* **1977**, *10*, 1229. Adam, M.; Delsanti, M. *Macromolecules* **1985**, *18*, 1760.
(17) Brown, W.; Štěpánek, P. *Macromolecules* **1993**, *26*, 6884. Brown, W.; Štěpánek, P. *Macromolecules* **1992**, *25*, 4359. Brown, W.; Štěpánek, P. *Macromolecules* **1988**, *21*, 1791.
(18) Koňák, Č.; Mrkvièková, L.; Bansil, R. *Macromolecules* **1996**, *29*, 6158.
(19) Brochard, F.; De Gennes, P. G. *Macromolecules* **1977**, *10*, 1157.
(20) Wang, C. H. *J. Chem. Phys.* **1991**, *95* (5), 3788.
(21) Wang, C. H. *Macromolecules* **1992**, *25*, 1524.
(22) Wang, C. H.; Fytas, G.; Fisher, E. W. *J. Chem. Phys.* **1985**, *82* (9), 4332.
(23) Wang, C. H.; Zhang, X. Q. *Macromolecules* **1993**, *26*, 707. Wang, C. H.; Zhang, X. Q. *Macromolecules* **1995**, *28*, 2288.
(24) Wang, C. H.; Sun, Z.; Huang, Q. R. *J. Chem. Phys.* **1996**, *105* (14), 6052.
(25) Adam, M.; Farago, B.; Schleger, P.; Raspaud, E.; Lairez, D. *Macromolecules* **1998**, *31*, 9213.
(26) Colby, R. H.; Rubinstein, M. *Macromolecules* **1990**, *23*, 2753.
(27) Nicolai, T.; Brown, W.; Johnsen, R. M.; Štěpánek, P. *Macromolecules* **1990**, *23*, 1165.
(28) Nicolai, T.; Brown, W. *Macromolecules* **1990**, *23*, 3150. Nicolai, T.; Brown, W. *Macromolecules* **1996**, *29*, 1698.
(29) Brown, W.; Johnsen, R. M. *Macromolecules* **1985**, *18*, 379.
(30) Xie, Y.; Ludwing, K. F.; Bansil, R.; Gallagher, P. D.; Cao, X.; Morales, G. *Physica A* **1996**, *232*, 94.
(31) Kostko, A. F.; Anisimov, M. A.; Sengers, J. V. *Phys. Rev. E* **2002**, *66*, 020803.
(32) Brown, W.; Johnsen, R. M.; Konak, C.; Dvoranek, L. *J. Chem. Phys.* **1991**, *95* (11), 8568.
(33) Nose, T.; Chu, B. *Macromolecules* **1979**, *12*, 590.
(34) Sawatari, N.; Yoshizaki, T.; Yamakawa, H. *Macromolecules* **1998**, *31*, 4218.
(35) Schröder, J. M.; Wiegand, S.; Aberle, L. B.; Kleemeier, M.; Schröer, W. *Phys. Chem. Chem. Phys.* **1999**, *1*, 3287.
(36) Appelt, B.; Meyerhoff, G. *Macromolecules* **1980**, *13*, 657.
(37) Chu, B. *Laser Scattering*, 2nd ed.; Academic Press: New York, 1991.
(38) Wu, C.; Zhou, S. Q. *Macromolecules* **1995**, *28*, 8381.
(39) Berne, B.; Pecroa, R. *Dynamic Light Scattering*; Plenum Press: New York, 1976.
(40) Bwown, W. *Light Scattering: Principles and Development*; Clarendon Press: Oxford, U.K., 1996.
(41) Provencher, S. W. *J. Chem. Phys.* **1978**, *69*, 4273.
(42) Adam, M.; Lairez, D.; Raspaud, E.; Fango, B. *Phys. Rev. Lett.* **1996**, *77*, 3673.
(43) Ngai, T.; Wu, C.; Chen, Y. *J. Phys. Chem. B* **2004**, *108* (18), 5532
(44) Brown, W. *Macromolecules* **1984**, *17*, 66. Brown, W. *Macromolecules* **1985**, *18*, 1713.
(45) Bastide, J.; Leibler, L. *Macromolecules* **1988**, *21*, 2647.
(46) Brown, W.; Mortensen, K. *Macromolecules* **1988**, *21*, 420.
(47) Colby, R. H.; Fetters, L. J.; Funk, W. G.; Graessley, W. W. *Macromolecules* **1991**, *24*, 3873.
(48) Nicolai, T.; Brown, W.; Hvidt, S.; Heller, K. *Macromolecules* **1990**, *23*, 5088.
(49) Vshivkov, S. A.; Safronov, A. P. *Macromol. Chem. Phys.* **1997**, *198*, 3015.
(50) Liu, Z.; Pan, C.; Lodge, T. P.; Stepanek, P. *Macromolecules* **1995**, *28*, 3221.
(51) Borsali, R.; Fischer, E. W.; Benmouna, M. *Phys. Rev. A* **1991**, *43-(10)*, 5732.
(52) Benmouna, M.; Benoit, H.; Borsali, R.; Duval, M. *Macromolecules* **1987**, *20*, 2620.
(53) Borsali, R.; Vilgis, T. A. *J. Chem. Phys.* **1990**, *93* (5), 3610.
(54) Jian, T.; Anastasiadis, S. H.; Semenov, A. N.; Fytas, G.; Adachi, K.; Kotaka, T. *Macromolecules* **1994**, *27*, 4762.
(55) Semenov, A. N.; Anastasiadis, S. H.; Boudenne, N.; Fytas, G.; Xenidou, M.; Hadjichristidis, N. *Macromolecules* **1997**, *30*, 6280.
(56) Chrissopoulou, K.; Pryamitsyn, V. A.; Anastasiadis, S. H.; Fytas, G.; Semenov, A. N.; Xenidou, M.; Hadjichristidis, N. *Macromolecules* **2001**, *34*, 2156.

(57) Anastasiadis, S. H.; Fytas, G.; Vogt, S.; Fisher, E. W. *Phys. Rev. Lett.* **1993**, *70* (16), 2415.
(58) Boudenne, N.; Anastasiadis, S. H.; Fytas, G.; Xenidou, M.; Hadjichristidis, N.; Semenov, A. N.; Fleischer, G. *Phys. Rev. Lett.* **1996**, *77* (3), 506.
(59) Painter, P. C.; Berg, L. P.; Veytsman, B.; Coleman, M. M. *Macromolecules* **1997**, *30*, 7529.
(60) Chang, B. H.; Bae, Y. C. *Polymer* **1997**, *38*, 4819.
(61) Li, X. Y.; Zhao, D. L. *J. Chem. Phys.* **2002**, *117* (14), 6803.
(62) Janssen, R. H. C.; Wang, S.; Nies, E. *Macromolecules* **1999**, *32*, 471.
(63) Painter, P. C.; Veytsman, B.; Kumar, S.; Shenoy, S.; Graf, J. K.; Xu, Y.; Coleman, M. M. *Macromolecules* **1997**, *30*, 932.
(64) Doi, M.; Onuki, A. *J. Phys. II* **1992**, *2*, 1631.
(65) Uematsu, T.; Svanberg, C.; Nyden, M.; Jacobsson, P. *Phys. Rev. E* **2003**, *68*, 051803.

MA071284B